

Preparation of an ultra-oriented polyethylene morphology

NUMA CAPIATI*, SHUNJI KOJIMA†, WILLIAM PERKINS,
ROGER S. PORTER

*Materials Research Laboratory, Polymer Science and Engineering, University of
Massachusetts, Amherst, Massachusetts, USA*

A technique for producing an ultra-drawn morphology for high-density polyethylene has been described previously. This technique has subsequently been extensively modified to produce the ultra-drawn morphologies under continuous and more versatile conditions. These changes involve using the reservoir of an Instron rheometer to prepare a crystal morphology prior to proceeding with a solid state (crystal-crystal transformation) extrusion process in the same instrument. The new preparation conditions are described to up-date the prior procedure and to document this new method which is now being employed in several laboratories to produce transparent polyethylene morphologies of extreme orientation and chain extension which results in filaments and films of extreme tensile moduli.

1. Introduction

The molecular chains of a crystalline linear polymer, when perfectly extended, can have a longitudinal stiffness similar to that of steel [1, 2]. However, commercial plastics usually exhibit tensile moduli from 20 to over 100 times lower [3]. Even for highly-oriented synthetic fibres the modulus will be relatively low unless a proportion of the chains are highly extended as it is the extended chains which provide the longitudinal continuity that leads to a high tensile modulus [4-7].

The methods available to obtain highly-oriented and extended-chain materials can be divided in two categories: those in which the flow or deformation is purely extensional [7-9] and those bearing an important shear component [10-13]. Peterlin [14] and Ziabicki [13] and, more recently, Frank and co-workers [1, 9] have emphasized the importance of the elongational deformation to achieve a considerable chain extension. In shear flow, the velocity gradient normal to the flow direction induces a superposed motion of rotation

and translation on each material element. This effect restricts the molecular extension achievable.

The concepts described here are substantially different from the alternative ways to promote orientation (drawing, spinning, solution-grown crystals under shear, etc). This report contains a description of the method we currently use. It differs from the procedure used previously in this laboratory by Southern, Weeks and by Niikuni both in the capillary geometry and in the conditions for crystallization prior to extrusion [15]. We currently reach an equilibrium crystallization before deformation is induced. We then perform a solid-state extrusion rather than one in a highly viscous liquid state. This minimizes the shear (rotational) flow and favours an elongational deformation which provides a higher efficiency for chain orientation and extension.

Our prior reports remain entirely valid as far as we know [15]. They may, nonetheless, be misleading since we have subsequently developed a much more efficient and, importantly, essentially continuous method for producing high-

*Present address: Planta Piloto de Ing. Qca., Universidad Nacional del Sur, Bahia Blanca, Argentina.

†Present address: The Composite Research and Development Center of Toyo Seikan and Toyo Kohan Companies, Yokohama, Japan.

density polyethylene strands of extreme orientation. We therefore offer this standard method which is now being used in several research laboratories including our own.

2. Methods

Strong, ultra-oriented strands and film strips of high-density polyethylene now can be extruded, free of defects and of indefinite length, in an Instron Capillary Rheometer. Pressure, temperature and capillary geometry are among the important parameters in preparation of the ultra-oriented morphologies. A typical material used is DuPont Alathon 7050 high-density polyethylene, $M_w = 59\,000$, $M_n = 20\,000$. Many other high-density polyethylenes have been shown amenable to these procedures, including Alathons with a range of molecular weights, and comparable samples from the Phillips Company.

The preparation procedure can be separated in three steps: (1) conditioning of the test specimens, (2) crystallization under pressure, and (3) morphological changes produced under solid-state high-pressure extrusion.

2.1. Preparation

The polyethylene is placed in the reservoir of an Instron rheometer and compacted in a conventional way at a temperature just below ($\sim 5^\circ\text{C}$), the polymer melting point. The plunger is placed into the rheometer barrel and a restrictor is placed at the base of the capillary. The restrictor is a simple, conically tipped steel needle which can be screwed firmly between the Instron base and the rheometer to plug the capillary. The temperature is then increased at atmospheric pressure up to around 170°C to melt the polyethylene. Next the heaters are shut off and the temperature reduced towards working conditions. When temperature nears the set point, the automatic temperature controller is switched on and temperature is allowed to stabilize.

2.2. Crystallization under pressure

Pressure is now increased by moving down the rheometer plunger with the Instron cross-head at a fixed speed (a typical value is 1 cm min^{-1}). When the working pressure is reached (e.g. 2400 atm), the cross-head speed is reduced gradually towards the minimum value (0.005 cm min^{-1}) to maintain a constant and high pressure, commonly near the upper limit of the Instron. For convenience, the

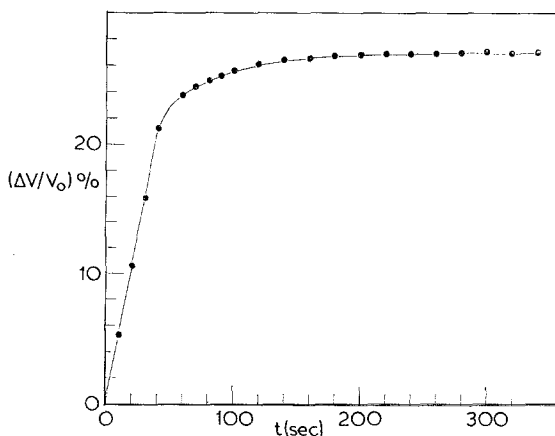


Figure 1 Volume decrease for polyethylene on increasing pressure to 2000 atm with time at 135°C .

instrument may be put on cyclic loading at a force corresponding to the desired pressure. The cross-head motion is stopped and started automatically in a close interval around the desired pressure. The crystallization is presumed to reach equilibrium when the volume reduction approaches zero, which is detected by pressure constancy with the cross-head still. Fig. 1 shows the volume change with time during a typical run at 135°C and 2000 atm . Pressure is increased from 1 to 2000 atm in the first 41 sec. Since the cross-head speed is constant, the change in volume is a linear function of time in this region. A plot of pressure versus time (Fig. 2) shows the onset of crystallization at about 500 atm . At this point a decrease in slope, corresponding to a lower resistance to volume change, indicates the crystallization initiation. Once the working pressure is reached, the cross-head speed is reduced gradually. Here the

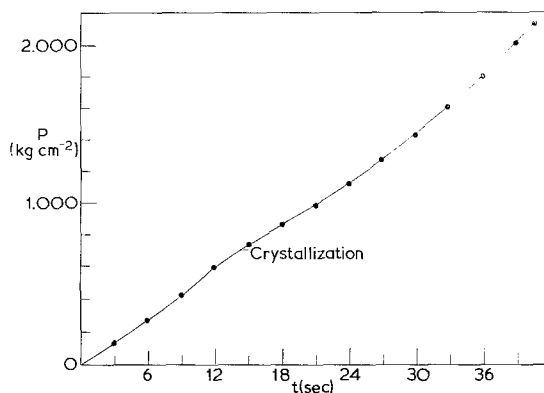


Figure 2 Change of pressure with time in the Instron rheometer showing crystallization of high-density polyethylene.

volume reduction slows down progressively with time beyond the linear region. As can be seen in Fig. 1, the volume change decreases rapidly and in relatively short time, about 100 sec, reaches an equilibrium value indicating the end of this step.

2.3. Morphology, preparation under stress and pressure during extrusion

The restrictor is taken off and extrusion initiated. A 600 g weight, clamped onto the end of the emerging fibre, keeps the fibre straight during the extrusion process. This weight is sufficiently small compared to the extrusion pressure that it does not increase the extrusion rate. The cross-head motion is periodically reset to maintain a constant, high and predetermined pressure near the Instron maximum. The subsequent morphological transformation during extrusion is achieved by the combined effect of pressure and tensile deformation in the capillary entrance region.

The flow rate is highest at the beginning in successful extrusions. Still at constant and high pressure, the flow slows down until a constant and slow rate of extrusion is reached. The first portions (~20 cm) of the extruded strands have lower perfection, i.e. lower melting points, heats of fusion, moduli and tensile strengths, than the subsequent portions. This is consistent with the idea of more perfect morphologies produced during steady extrusion at higher draw ratios.

3. Discussion

The method described above differs in two essential ways from our former published procedure [15].

(1) *The use of a restrictor with the consequent result of a two-stage process for morphology preparation.* Niikuni and earlier workers on this project crystallized polyethylene directly from the melt, inducing the first nuclei by shear stress plus some pressure. Pressure increased abruptly in this former process only when the flow was arrested by extensive crystallization in shear. With the present method, pressure is imposed before any crystallization takes place and the first stage of crystallization is carried out at the working pressure but without shear. This produces an equilibrium, spherulitic morphology at an undercooling corresponding to the elevation of melting point due to pressure of about 20°C per 1000 atm [16]. The polymer is subsequently extruded and the second

TABLE I Capillaries used for solid state extrusion

Entrance angle (deg)	Diameter (cm)	Length cylindrical part (cm)
90	0.150	0.70
40	0.155	0.80
30	0.135	0.60
20	0.135	1.50

stage of morphology preparation, i.e. the crystal-crystal transformation, is induced.

(2) *The capillary geometry.* Niikuni used only capillaries of 90° entrance angle. The best results were subsequently obtained here using a capillary of 20° included angle. The former capillary lengths used formerly were relatively large (the shortest being 2.5 cm whereas lengths smaller than 2 cm now appear to be desirable for the production of long strands of good perfection for ultra-oriented polyethylene. Capillary length itself, however, may not be a sensitive variable in these studies. Table I shows the dimensions of capillaries that have now been tried.

3.1. Calculations of deformation intensity

At the early stages of extrusion, the effective radius, R_a , of the entrance zone at each stage of deformation can be calculated. Equating the volume of the truncated entrance zone cone to the volume of extruded fibre gives (see Fig. 3):

$$(R_a^3 - R_b^3)/3 \tan \theta = R_b^2 \cdot L$$

or

$$R_a = (R_b^3 + 3L \cdot R_b^2 \tan \theta)^{1/3} \quad (1)$$

where R_a is the effective radius before deformation, R_b the radius of capillary, and θ the cone half angle.

The actual draw ratio (DR) may be calculated assuming volume conservation as a function of fibre length, L , by substituting Equation 1 into

$$\begin{aligned} \text{DR} &= (R_a/R_b)^2 \\ &= (1 + 3L \frac{1}{R_b} \tan \theta)^{2/3}. \end{aligned} \quad (2)$$

The calculations of DR for several capillaries of constant entrance angle are shown in Fig. 4 as a function of extruded fibre length, L . The value of DR gives the total amount of deformation applied at each polymer.

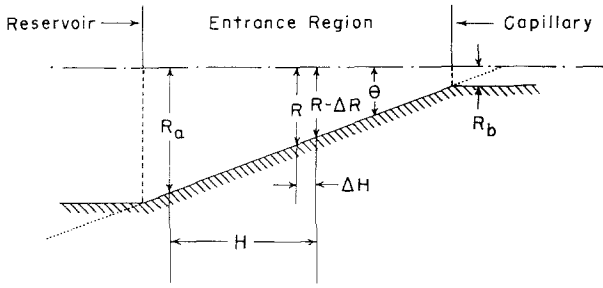


Figure 3 Cross-section of conical entrance region of capillaries.

Maximum Deformation Intensity Defined

$$d[DR]/dH = 2R_a^2 \tan \theta / R_b^3$$

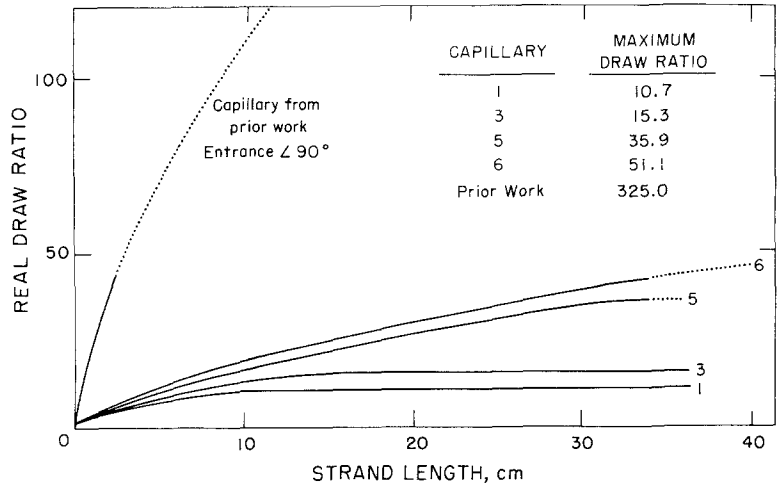


Figure 4 Real draw ratio as a function of strand length.

We now define the distance, H , between the points where the radius is R_a and R from the geometric relationship,

$$H = (R_a - R) / \tan \theta. \quad (3)$$

We can thus write the draw ratio between these points as follows:

$$DR = (R_a / R)^2, \quad (4)$$

and combining with Equation 3 gives

$$DR = [R_a / (R_a - H \tan \theta)]^2. \quad (5)$$

Differentiating with respect to H gives

$$\begin{aligned} \frac{d(DR)}{dH} &= \frac{2R_a^2 \tan \theta}{(R_a - H \tan \theta)^3} \\ &= 2R_a^2 \tan \theta / R^3. \end{aligned} \quad (6)$$

The value $d(DR)/dH$ is a rate change of draw which reaches a maximum at the cone exit. That is, from Equation 6, the maximum is

$$\begin{aligned} \left[\frac{d(DR)}{dH} \right]_{\max} &= \left[\frac{d(DR)}{dH} \right]_{R=R_b} \\ &= 2R_a^2 \tan \theta / R_b^3. \end{aligned} \quad (7)$$

Substitution of Equation 1 into Equation 7 gives

$$\left[\frac{d(DR)}{dH} \right]_{\max} = 2 \tan \theta \left(1 + 3L \frac{1}{R_b} \tan \theta \right)^{2/3} \quad (8)$$

which is the maximum deformation intensity.

On the other hand, from the assumption of non-compressive volumetric flow,

$$V_a \cdot R_a^2 = V \cdot R^2$$

where V_a and V are velocities of material at R_a and R . Therefore, solving for V and substituting:

$$V = V_a (R_a / R)^2 = V_a \cdot (DR). \quad (9)$$

TABLE II Maximum draw ratio and deformation intensity for capillaries of constant entrance angle

Capillary	Maximum draw ratio	Maximum deformation intensity (cm^{-1})
1	10.7	25.9
2	11.8	30.1
3	15.3	44.6
4	24.8	92.2
5	35.9	160.4
6	51.1	271.9
By Southern	325	4365

Differentiation of Equation 9 with respect to H gives

$$\frac{dV}{dH} = V_a \frac{d(\text{DR})}{dH} \quad (10)$$

Equation 10 gives the relationship between deformation intensity and extensional shear rate.

Results calculated for capillaries used in this study and by Southern are shown in Table II. It is shown that the deformation intensity of the capillary used by Southern is 100 times as high as for those capillaries used here.

It has been possible to achieve a continuous extrusion for capillaries 1 to 4 which have a lower maximum deformation intensity (see Table II). Thus, it is desirable to design a capillary which has low deformation intensity to obtain fibres with the highest draw ratio.

For design for a zone of constant deformation intensity:

$$\frac{d(\text{DR})}{dH} = C \quad (11)$$

where C is a constant. Integration gives

$$\text{DR} = C \cdot H + C_0$$

where C_0 is a constant equal to 1.0 because $\text{DR} = 1.0$ where $H = 0$. Therefore,

$$\text{DR} = C \cdot H + 1. \quad (12)$$

On the other hand, by cylindrical symmetry, Equation 4 is valid here. Combining Equations 4 and 12

$$\begin{aligned} (R_a/R)^2 &= C \cdot H + 1 \\ R &= R_a/\sqrt{(CH + 1)}. \end{aligned} \quad (13)$$

Two designs with R_a of 0.4735 cm are plotted for $C = 20$ and 30 cm^{-1} in Fig. 5. It is thus possible

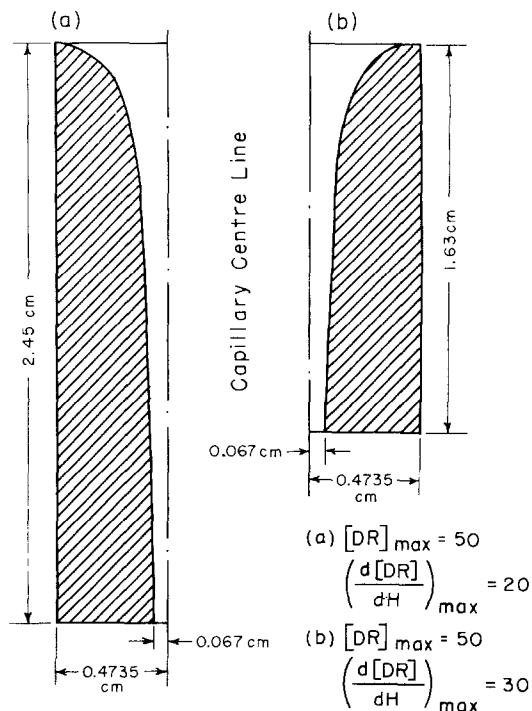


Figure 5 Cross-sections for capillaries designed for constant deformation intensity for Instron Rheometer.

to attain a high draw ratio at a lower deformation intensity (cf. Table II).

The importance of this factor, deformation intensity, is that: (1) it is a comparable factor to extensional shear rate, (2) it is simpler than extensional shear rate because it is not velocity (time) dependent, and (3) solution of Equation 11 is simpler and wider than that from $dV/dH = C$, i.e. the latter is involved in Equation 13.

3.2. Comments on capillary geometry

The lengths of extrudable strands, free of defects, that can be obtained are very sensitive to the cleanliness and smoothness of the inner surface of the capillary and entrance region. Lubrication with Teflon spray (bonding grade) proved to be useful. The Teflon adheres to the capillary wall forming a very thin layer with an extremely low friction coefficient. The application of the Teflon is done by spraying against the entrance zone while pulling a vacuum on the back (capillary) end. The Teflon coating is also buffed in.

Long strands, over 14 in. (35 cm), of clear, strong polyethylene are obtained using a brass capillary of draw ratio 52 with 20° entrance angle, polished and Teflon lubricated. With cap-

illaries of lower draw ratio, the extrusion is essentially continuous.

Both entrance angle and draw ratio influence the maximum strand length achievable before fracture starts to appear. Experiments developed with different entrance angles for capillaries of the same length and diameter show a consistent increase in strand length with a reduction of angle. The smallest angle tried was 20°. However, this is probably greater than the optimum. This is because of the lower maximum deformation intensity at the lower entrance angle (see Equation 7). Predecki and Statton [17] for example, proposed that the best value would be around 4°.

Explanation of the improvement in strand quality with angle reduction might be based on the longer residence time under deformation in the cone region. With such a slower rate of draw there is a more gradual development of shear and/or tensile stress. Equation 13 shows that a trumpet-shaped entrance region might be the optimum contour for maximizing the deformation intensity. A small angle, and certainly lubrication, may also shift the ratio of shear and tensile stress in the favorable direction of more tensile stress, i.e. more extensional flow. The residence time in the capillary cone entrance must thus be equal or longer than the natural time for conversion from folded to extended chain morphology and thus will involve a rate process which may well be exceeded at rapid extrusion rates. The Niikuni tests showing onset of fracture at different draw ratios seem to bear this out [15].

The influence of capillary diameter and length is less evident. They appear to play a role in controlling the pressure level and gradient in the entrance cone. Neglecting axial pressure differences in the reservoir, the total pressure drop is developed both in the conical and the cylindrical regions of the capillary. Larger capillary diameters and/or longer conical (entrance) portions make the pressure drop increasingly more important in the entrance cone relative to the cylindrical (capillary) region. This seems to produce more perfect strands. It thus may be that the morphological transformation may be influenced more by the pressure difference than the absolute pressure.

3.3. Possibilities of this method

An interesting alternative to these procedures involves crystallization at higher temperatures.

With the previous method used by Niikuni and Weeks, it is not possible to reach enough shear stress to allow massive crystallization above 137°C. Thus strands produced up to now have been extruded at temperatures no higher than 136°C and 2400 atm pressure. By the following method, there is no temperature limitation. The equilibrium melting point at 2000 atm pressure for linear polyethylene is near 168°C [16]. Therefore, assuming a 135°C operation temperature, the supercooling is 33°C. This relatively high supercooling leads to a rapid crystallization in the reservoir, but the crystal thickness will be quite small. With a supercooling of 15°C, primary crystallization is completed in about 30 min. [18]. Furthermore, the increase in lamellar thickness with reduction of supercooling is remarkable (for example, 65% increase on passing from 33 to 15°C supercooling). Apparently we can obtain considerably thicker crystals by operating at 150°C (18°C supercooling) during the first stage of crystallization, and the crystallization time will not be unreasonably large (not much longer than 30 min). Once crystallized at 150°C and 2000 atm, either the temperature can be reduced at 135°C and the extrusion started, or the material can be extruded at 150°C using a cooling system at the exit to avoid the strand melting. This interesting experiment has not yet been done. Indeed, we await a major area of research which will involve decoupling the pressure effects on morphology preparation and on extrusion rate. Our basic method now allows us to prepare crystals under a variety of conditions prior to extrusion.

References

1. F. C. FRANK, *Proc. Roy. Soc. Lond. A* **319** (1970) 127.
2. I. SAKURADA and K. KAJI, *J. Polymer Sci. C* **31** (1970) 57.
3. J. BANDRUP and E. H. IMMERGUT, "Polymer Handbook" (Interscience, New York, 1966).
4. R. S. PORTER, Symposium on Unsolved Problems in Polymer Science, ACS Meeting, Washington, D.C. (1971).
5. A. PETERLIN, *J. Mater. Sci.* **6** (1971) 490.
6. A. PETERLIN, *Textile Res. J.* **42** (1972) 20.
7. N. J. CAPIATI and R. S. PORTER, *J. Polymer Sci. Polymer Phys. Ed.* **13** (1975) 1177.
8. T. T. WANG, H. S. CHENG and T. K. KWEI, *J. Polymer Sci. B* **8** (1970) 505.
9. F. C. FRANK, A. KELLER and M. R. MACKLEY, *Polymer* **12** (1971) 467.

10. K. IMADA, T. YAMAMOTO, K. SHIGEMATSU and M. TAKAYANAGI, *J. Mater. Sci.* **6** (1971) 537.
11. A. J. PENNING, *J. Polymer. Sci.* **16** (1967) 1799.
12. A. J. PENNING and A. M. KIEL, *Koll. Z. Polym.* **205** (1965) 160.
13. A. ZIABICKI, *J. Appl. Polymer. Sci.* **2** (1959) 24.
14. A. PETERLIN, *J. Polymer. Sci. B.* **4** (1966) 287.
15. T. NIKUNI and R. S. PORTER, *J. Mater. Sci.* **9** (1974) 389.
16. B. WUNDERLICH and T. ARAKAWA, *J. Polymer. Sci. A.* **2** (1964) 3697.
17. P. PREDECKI and W. O. STATTON, *ibid.*, **B.** **10** (1972) 87.
18. P. D. CALVERT and D. R. UHLMANN, *ibid.*, **A-2** **10** (1972) 1811.

Received 22 April and accepted 21 May 1976.